Electron Transfer in Photosystem I Reaction Centers Follows a Linear Pathway in Which Iron −Sulfur Cluster F B Is the Immediate Electron Donor to Soluble Ferredoxin †

ARTICLE *in* BIOCHEMISTRY · MARCH 1998

Impact Factor: 3.02 · DOI: 10.1021/bi972469l · Source: PubMed

4 AUTHORS, INCLUDING:

Antonio Díaz-Quintana
Universidad de Sevilla
70 PUBLICATIONS **987** CITATIONS
SEE PROFILE

Winfried Leibl
Atomic Energy and Alternative Energies Com…
78 PUBLICATIONS **1,966** CITATIONS
SEE PROFILE

Herve Bottin
Atomic Energy and Alternative Energies Com…
59 PUBLICATIONS **1,663** CITATIONS
SEE PROFILE

Electron Transfer in Photosystem I Reaction Centers Follows a Linear Pathway in Which Iron−Sulfur Cluster F_B Is the Immediate Electron Donor to Soluble Ferredoxin†

A. Díaz-Quintana,‡ W. Leibl, H. Bottin, and P. Sétif*

CEA, Département de Biologie Cellulaire et Moléculaire, Section de Bioénergétique, CNRS, URA 2096, C.E. Saclay, 91191 Gif sur Yvette Cedex, France

Received October 6, 1997; Revised Manuscript Received December 23, 1997

ABSTRACT: Reaction centers of photosystem I contain three different [4Fe-4S] clusters named F_X, F_A, and F_B. The terminal photosystem I acceptors (F_A, F_B) are distributed asymmetrically along the membrane normal, with one of them (F_A or F_B) being reduced from F_X and the other one (F_B or F_A) reducing soluble ferredoxin. In the present work, kinetics of electron transfer has been measured in PSI from the cyanobacterium *Synechocystis* sp. PCC 6803 after inactivation of F_B by treatment with $HgCl_2$. Photovoltage measurements indicate that, in the absence of F_B, reduction of F_A by F_X is still faster than the rate of F_X reduction [$(210\ ns)^{-1}$]. Flash-absorption measurements show that the affinity of ferredoxin for $HgCl_2$-treated PSI is only decreased by a factor of 3−4 compared to untreated photosystem I. The first-order rate of ferredoxin reduction by F_A^-, within the photosystem I/ferredoxin complex, has been calculated from measurements of $P700^+$ decay. Compared to control PSI, this rate is several orders of magnitude smaller (6 s^{-1} versus 10^4−10^6 s^{-1}). Moreover, it is smaller than the rate of recombination from F_A^-, resulting in inefficient ferredoxin reduction (yield of 25%). After reconstitution of F_B, about half of the reconstituted photosystem I reaction centers recover fast reduction of ferredoxin with kinetics similar to that of untreated photosystem I. These results support F_B as the direct partner of ferredoxin and as the more distal cluster of photosystem I with respect to the thylakoid membrane, in accordance with a linear electron-transfer pathway $F_X \rightarrow F_A \rightarrow F_B \rightarrow$ ferredoxin.

In oxygenic photosynthetic organisms, the reduction of soluble ferredoxin (Fd)[1] is catalyzed by photosystem I (PSI) by means of a multistep charge separation and stabilization process (for reviews, see refs 1, and 2). Such a process first involves a photoinduced charge separation between the primary donor P700 and the primary acceptor A_0, both being chlorophyll molecules. This initial reaction is followed by electron transfer from A_0 to a phylloquinone molecule named A_1 and to later reduction of iron−sulfur clusters by A_1^-. The terminal acceptors F_A and F_B, which are two [4Fe-4S] clusters bound to the stromal PsaC subunit of PSI, are eventually reduced most probably by F_X, a third [4Fe-4S] cluster bound to the heterodimeric core protein PsaA/PsaB of PSI (*3*−*5*). The X-ray structure of PSI, which is presently known at 4 Å resolution (*6*), has shown that the axis joining F_A and F_B is tilted out of the membrane plane by an angle of 36° (*7*). Subunit PsaC exhibits some sequence homology to bacterial 2[4Fe-4S] ferredoxins, especially in the cysteine binding motifs. The structures of four such bacterial ferredoxins have been determined (*8*−*11*).

The ferredoxin structure of *Peptococcus aerogenes* has been used to model PsaC into the electron density map of PSI (*12*) and the orientations of the EPR F_A^- and F_B^- **g**-tensors were determined (*13*). Assignment of F_A and F_B to their respective ligands has been derived from directed modifications of cysteine residues (*14*−*19*). Taken together, all these data should in principle allow identification of the respective positions of F_A and F_B, i.e., which cluster is proximal (or distal) to the membrane plane. However, there is still ambiguity in this assignment due to the lack of atomic resolution and to local pseudosymmetry of subunit PsaC (*12*). Moreover, directed modifications of cysteine ligands in *Synechocystis* sp. PCC 6803 (*18*, *19*) or with a reconstituted system involving modified PsaC (*14*−*16*) did not help in assigning the positions of F_A and F_B in the PSI complex. This was due to the fact that only PsaC containing two [4Fe-4S] clusters was stably assembled into PSI, leading to the presence of a mixed-ligand cluster in the mutant forms with functional properties similar to that of the wild-type cluster. By contrast, directed modification of a cysteine ligand in *Anabaena variabilis* purportedly led to the absence of cluster F_B in PSI (*17*), though this has been questioned recently (*18*).

Following initial experiments (*20*), the functional effects of the selective destruction of F_B by $HgCl_2$ were studied by

† This work was supported in part by an institutional grant from the European Commission (Human Capital and Mobility program, contract ERBCHBG CT 93−0389) (A.D.-Q).

* To whom correspondence should be addressed.

‡ Present address: Instituto de Bioquimica Vegetal y Fotosintesis, C.I.C. Isla de la Cartuja, Avda. Americo Vespucio, 41092 Sevilla, Spain.

[1] Abbreviations: Fd, ferredoxin; PSI, photosystem I; F_X, F_A, F_B, iron−sulfur clusters of photosystem I; OGP, octyl-β-D-glucopyranoside; β-DM, β-dodecyl maltoside; DCPIP, 2,6-dichlorophenolindophenol.

S0006-2960(97)02469-0 CCC: $15.00
Published on Web 02/20/1998

various groups (*21*−*25*). It was found that F_B disruption inactivates $NADP^+$ photoreduction, whereas the yield of F_A photoreduction was not affected both at room temperature and low temperature. Moreover, $NADP^+$ photoreduction has been successfully restored after reconstitution of F_B (*23*, *25*), thus pointing out the indispensable role of F_B in forward electron transfer to Fd. Together with the larger sensitivity of F_B toward oxidative destruction (*26*), this supports the view that F_B is the most distal cluster. This is in accordance with a linear electron-transfer pathway from F_X to Fd assuming that the distal cluster is the immediate electron donor to Fd, as was recently concluded both from modeling of the PSI/Fd complex (*27*) and from a microscopy study of a covalent complex (*28*). However, it cannot be excluded that destruction of F_B has some structural effects sufficient for strongly disturbing Fd docking. If one assumes that F_B is the cluster which is proximal to F_X, destruction of F_B could lead for example to a considerable decrease in the efficiency of Fd reduction by F_A, despite the fact that F_A can be reduced efficiently directly from F_X. Though rather unlikely, such a possibility would be in line with two recent studies based on reconstitution experiments involving subunit PsaC, which was modified by mutagenesis. Using in one case a modified PsaC lacking either an internal loop or 10 residues of the C terminus (*29*) and, in another case, site-directed mutants of PsaC with replacement of acidic residues (*30*), both studies favor F_B as the proximal cluster. These uncertainties prompted us to perform a detailed kinetic characterization of PSI reaction centers from the cyanobacterium *Synechocystis* sp. PCC 6803 which have lost cluster F_B after treatment with $HgCl_2$ together with experiments involving reaction centers with reconstituted F_B. We apply both photovoltage measurements for recording electron transfer within PSI and flash-absorption spectroscopy to characterize Fd reduction. Our data indicate that F_B is the distal cluster and is the direct partner of Fd in the frame of a linear electron-transfer pathway.

MATERIALS AND METHODS

Biological Materials. *Synechocystis* sp. PCC6803 was grown in BG 11 liquid media. Cells were harvested in the late logarithmic growth phase. Octyl β-D-glucopyranoside (OGP) membranes were obtained as previously described (*31*). For later use, these preparations were stored at −80 °C in the presence of 20% glycerol at a concentration of 2 mg of chlorophyll/mL. Fd from *Synechocystis sp*. PCC 6803 was isolated and purified according to ref 32. PSI from the same strain was isolated and purified in trimeric states with the detergent β-dodecyl maltoside (β-DM) as described in refs *33* and *34*. Chlorophyll concentration was determined by acetone extraction, according to ref *35*. P700 content was calculated from photoinduced absorption changes at 820 nm, assuming an absorption coefficient of 6500 M^{-1} cm^{-1} for $P700^+$ (*36*).

Chemical Treatments. Chemical core extrusion of center F_B was performed according to ref 21 with some modifications. PSI trimers (0.2 mg of chlorophyll/mL) were incubated either in the presence or in the absence (control) of 2.5 mM $HgCl_2$ in 50 mM Bis-Tris-propane/HCl, pH 8.5, 20 mM $CaCl_2$, 0.4 M sucrose, and 0.03% β-DM for 30 min at room temperature. The reaction was stopped by the addition of EDTA, pH 8, at a final concentration of 10 mM. Then the samples were concentrated with a Centriprep 100 filter (Amicon) and applied on a P4 gel filtration column (Bio Rad) equilibrated with 10 mM Bis-Tris-propane/HCl, pH 8.5, 0.03% β-DM. Finally, samples were washed and concentrated with 10 mM Tricine, pH 8, 0.03% β-DM with the Centriprep system. For OGP membranes, the treatment was performed at pH 9.3 under the same conditions. After incubation, 10 mM EDTA was added and the membranes were washed twice in 10 mM MES, pH 6.5. To quantify the fractions of centers with intact or destroyed F_A and F_B centers, samples were tested by laser flash-induced absorption changes at 820 nm as well as by low-temperature EPR. Extraction of F_A and F_B from OGP PSI membranes was performed with urea according to ref 37. Reconstitution experiments were performed on β-DM $HgCl_2$-treated samples, similarly to ref 38. A solution containing 50 mM Bis-Tris-propane/HCl, pH 8.5, 20 mM $CaCl_2$, 0.4 M sucrose, and 1 mM $FeCl_3$ was made oxygen-free by three cycles of alternative vacuum and argon flow. $HgCl_2$-treated PSI was put under anaerobiosis by flushing argon and then added to the first solution with β-DM at final concentrations of 0.2 mg of chlorophyll/mL and 0.03%, respectively. Then β-mercaptoethanol and Na_2S (from a fresh anaerobic solution) were added to final concentrations of 0.5% and 1 mM, respectively. The reaction mixture was incubated overnight and then exposed to air; 10 mM Tiron was then added to the reaction mixture. The resulting solution was then washed several times with 10 mM Tricine, pH 8, 0.03% β-DM in a Centriprep 100 filtration cell, concentrated, applied to a Bio Rad P4 gel filtration column equilibrated in the same buffer, and concentrated again.

Photoelectric Measurements. Photoinduced changes in electrogenicity of electrically oriented OGP membranes were performed as previously described (*39*). Signals were recorded with a bandwidth of 500 MHz on a digital storage oscilloscope (TDS 744A, Tektronix). All measurements were performed at room temperature. All samples were assayed under the same conditions in 5 mM MES, pH 6.5, and in the presence of 5 mM sodium ascorbate and 100 μM phenazine methosulfate.

EPR and Flash-Absorption Spectroscopies. Spectra were measured in a Bruker ESR300D X-band spectrometer equipped with an Oxford Instruments helium cryostat. Spectra of PsaC iron−sulfur clusters were recorded at 20 K, using a microwave power of 20 mW (nonsaturating conditions) and a modulation amplitude of 10 G at 100 kHz. Calibrated tubes were always used. EPR of fully reduced iron−sulfur clusters were obtained by preparing an anaerobic solution of PSI at a final concentration of 1 mg of chlorophyll/mL in 50 mM glycine/NaOH, pH 10, 0.03% β-DM to which dithionite was added in excess (10 mM final concentration). This solution was frozen at 200 K in the EPR tube under illumination. Light-induced spectra were obtained with samples in Tricine, pH 8, 0.03% β-DM, prepared in the presence of 2 mM sodium ascorbate and 50 μM DCPIP. These samples were incubated in darkness for 2 min before freezing in darkness and were illuminated at 20 K for 1 min. Kinetics of $P700^+$ decay was monitored at 820 nm. Kinetics of Fd reduction by PSI was recorded and analyzed as previously described (*40*, *41*).

Table 1: EPR Measurements and Characteristics of Flash-Induced Absorption Changes in Control, $HgCl_2$-Treated, and Reconstituted PSI[h]

method of characterization	control PSI	$HgCl_2$-treated PSI	reconstituted PSI
quantitation of spins by EPR			
spin amounts due to (F_A^-, F_B^-) or F_A^- in fully reduced samples (percents of control)	100	37	55
amounts of F_B^- in fully reduced samples (percents of control)	100	<3	50
amounts of F_A^- in photoinduced signals (percents of control)[a]	100	70	60
$P700^+$ decay at 820 nm		5 μs (15)	5 μs (15)
halftimes (percents of amplitude)	< 1 ms (<1)	75 μs (3)	75 μs (4)
		900 μs (12)	900 μs (17)
	> 10 ms (>99)	> 10 ms (70)	> 10 ms (64)
ferredoxin reduction			
halftimes at 480 nm (percents of amplitude)	*b*		
	< 1 μs (25)	nd	<1 μs (32)
	13−20 μs (22)		10 μs (24)
	110 μs (53)		70 μs (25)
dissociation constant	0.4−0.6 μM[(b)]	1.6 μM[(c)]	0.3 μM
slow decay of $P700^+$ in the absence of Fd[d]			
k_{obs} of slow component	16.6 s^{-1}	11.0 s^{-1}	14.0 s^{-1}
k_e/k_r ratio = ratio of amplitudes (very slow component/slow component)	0.89	0.07	0.82
deduced escape rate k_e	7.8 s^{-1}	0.7 s^{-1}	6.3 s^{-1}
deduced recombination rate k_r	8.8 s^{-1}	10.3 s^{-1} [e]	7.7 s^{-1}
slow decay of $P700^+$ in the presence of 2 μM Fd[d]			
k_{obs} of slow component	nd	22 s^{-1}	19 s^{-1}
$(k_e+k_tp)/k_r$ ratio = ratio of amplitudes (very slow component/slow component)[f]	>100	0.25	4.9
deduced rate $k_e + k_tp$	*g*	4.4 s^{-1}	ph
deduced recombination rate k_r	nr	17.6 s^{-1}	ph
calculated electron-transfer rates within the PSI/Fd complex[d]			
rate of Fd reduction k_t	see above (480 nm)	6.3 s^{-1}	see above (480 nm)
recombination rate k_{rcompl}	−	22.1 s^{-1} [e]	−

[a] + some minor F_B- signal in the control and reconstituted samples. [b] From refs 40 and 41. [c] Deduced from $P700^+$ decay at 820 nm. [d] One second full time scale. [e] Recombination between $P700^+$ and F_A-. [f] p, proportion of PSI reaction centers which bind Fd. [g] Cannot be determined from $P700^+$ decay. [h] nd: not detectable; nr: no recombination; ph: the rates cannot be calculated due to population heterogeneity (see the text).

RESULTS

Characterization of PSI after Removal and Reconstitution of F_B. F_B was removed by incubation with $HgCl_2$ from either β-DM or OGP PSI particles isolated from *Synechocystis* 6803. The reaction was performed under different salt and pH conditions for improving the yield of intact F_A clusters. Noteworthy, $HgCl_2$ reacts very slowly with the iron−sulfur cluster when added at submillimolar concentrations, possibly due to a chelating effect of the buffer. Native PSI (traces a), $HgCl_2$-treated (traces b), and reconstituted PSI (traces c) were characterized by both EPR (Table 1) and flash-absorption spectroscopy (Figure 1). In both cases, identical concentrations of PSI were used so that the respective signals could be directly compared. Low-temperature EPR spectra of fully reduced samples were recorded under conditions which allow quantitation of the amount of spins corresponding to F_A^- and F_B^-, when present. Whereas native PSI exhibit spectral features characteristic of the coupled spin system (F_A^-, F_B^-), only F_A^- is observable in $HgCl_2$-treated PSI (not shown): besides its typical g_y and g_z values of 1.94 and 2.05, a slightly shifted g_x signal is observed at 1.84 (instead of 1.86). A similar shift has been previously reported after treatment with $HgCl_2$ (*22*). As observed previously, F_B is completely absent after treatment (less than 3% as estimated from the signal-to-noise ratio of the EPR signal). When normalized to the P700 concentration, the amount of spins due to F_A^- in the $HgCl_2$-treated sample corresponds to 38% of the amount of spins due to (F_A^-, F_B^-) in the native reaction center, which means that about 75% of F_A is retained after the treatment. These numbers are

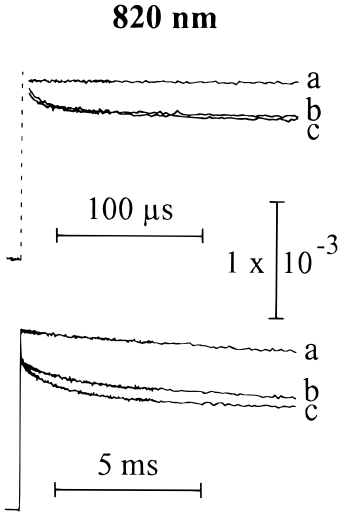

FIGURE 1: Flash-induced absorption changes measured at 820 nm with PSI trimers: control (a), treated with $HgCl_2$ (b), and reconstituted (c). All kinetics were normalized to a PSI concentration of 0.23 μM (concentration calculated from the initial amplitude at 820 nm given by a multiexponential fit and an absorption coefficient of 6500 M^{-1} cm^{-1}). Samples were prepared in 20 mM Tricine, pH 8.0, 30 mM NaCl, 5 mM $MgCl_2$, 0.03% β-DM, 1.3 mM sodium ascorbate, 9 μM DCPIP. Each trace is the average of 8 experiments (1 flash every 15 s). Kinetics are shown on two different time scales: upper part 200 μs (flash time is indicated by a vertical dotted line) and lower part 10 ms.

consistent with photoinduced signals measured at 20 K with samples prepared in the presence of ascorbate and frozen down to 20 K in darkness: in the $HgCl_2$-treated sample, the photoinduced F_A^- signal corresponds to about 70% of the photoinduced signal (F_A^- + some F_B^-) observed in the control sample.

$P700^+$ decay can be monitored by measuring flash-induced absorption changes at 820 nm at room temperature (Figure 1). Native PSI exhibits a very slow decay which is hardly visible on a 10 ms time scale (lower part). This is indicative of a very slow recombination reaction involving the terminal acceptors (F_A, F_B). By contrast, part of the decay is much faster in the $HgCl_2$-treated sample. This partial decay can be satisfactorily fitted with three kinetic components ($t_{1/2}$ of 5, 75, and 900 μs) and accounts for 30% of the initial absorption change (Table 1). Experiments made at 820 nm with a nanosecond time resolution indicate the absence of nanosecond components both in the control and $HgCl_2$-treated samples (Brettel and Diaz-Quintana, unpublished observations). This shows that a recombination reaction within the primary radical pair ($P700^+-A_0^-$) does not occur, in line with the presence of at least a secondary acceptor in all reaction centers. The 5 and 75 μs phases (18% of initial amplitude) can be ascribed to a recombination reaction between $P700^+$ and A_1^- in reaction centers devoid of F_A, F_B, and F_X (*42*, *43*). The 900 μs phase (12% of initial amplitude) can be assigned to reaction centers without (F_A, F_B) which undergo a recombination reaction between $P700^+$ and F_X^- (*44*). These data indicate that, besides F_B destruction, partial inactivation of F_A and F_X has occurred in 30% of the reaction centers and that 70% of $HgCl_2$-treated PSI retain a functional terminal acceptor F_A, in accordance with EPR measurements.

Reconstitution of F_B was carried out by reduction of cysteines (*45*) in the presence of sulfide and iron, which was added before β-mercaptoethanol (*46*). After reconstitution, $P700^+$ decay is practically unchanged with a slight decrease of the slower component (64%, $t_{1/2} > 10$ ms) indicative of a little further F_A destruction during the reconstitution treatment (Figure 1, 19% of 5 and 75 μs phases and 17% of 900 μs phase; Table 1). There is no evidence for any recombination between $P700^+$ and A_0^-, similar to the $HgCl_2$-treated sample (Brettel and Diaz-Quintana, unpublished observations). Despite the slight loss of F_A during reconstitution, a large fraction of F_B was reconstituted, as can be seen from the EPR spectrum, which resembles that of native PSI despite a smaller signal size (not shown). Spectral analysis and spin quantification shows that 50% of PSI contain both F_A and F_B after reconstitution, while about 40% are devoid of both centers. The remaining 10% of PSI exhibit only the F_A- signal (see also Table 1). When iron was added after reducing the cysteines following previous studies (*24*, *45*), no significant loss of F_A was observed during reconstitution, but only 30% of F_B was reconstituted (data not shown). This observation is in accordance with a previous report (*24*).

In the following, only slowly relaxing $P700^+$ (with at least F_A present) will be considered for estimating the amount of PSI reaction centers transferring electrons to Fd. This is justified by the fact that the microsecond recombination phases are not modified (in amplitude and kinetics) by the addition of Fd and by the previous observation that there is no direct electron transfer from F_X to Fd (*47*).

Direct Measurement of Fd Reduction by Reconstituted PSI. Electron transfer from native PSI to Fd was monitored by following the absorption changes due to Fd reduction at 480 and 580 nm (*40*, *41*). On a 1 ms time scale, only a very small signal is observed at both wavelengths with F_B-depleted PSI and 2 μM Fd, as is shown for 480 nm in trace b of Figure 2. The same small signal is observed at higher Fd concentrations (not shown). It may be ascribed to a very small change in the absorption properties of F_A when Fd is bound (see below) which results in such a steplike signal when the difference between signals with and without Fd is calculated (*41*). By contrast, a much larger signal is observed with reconstituted PSI (trace c). The signal amplitude found in the reconstituted sample corresponds to approximately half of the amplitude found in the control sample (trace a; see below). The three signals can be directly compared as they were obtained at similar Fd concentrations and identical amounts of slowly relaxing $P700^+$ (containing at least one terminal acceptor F_A or F_B). The signal found with reconstituted PSI exhibits fast kinetics which is completed after a few hundred microseconds. These kinetics include a fast unresolved component ($t_{1/2} < 1$ μs) observed both at 480 and 580 nm (32% and 49% of the total amplitudes, respectively) and a microsecond component. This component can be fitted by a single exponential phase with a halftime of 34 μs, but is better fitted with two exponential phases with halftimes of 10 and 70 μs, respectively (amplitudes in approximately a 1/1 ratio; Table 1). Such a kinetic behavior is very similar to that observed in untreated PSI, in which the existence of three phases with halftimes of approximately 0.5, 15, and 100 μs has been previously documented (*41*).

Reduction of Fd in reconstituted samples was also measured at 580 nm at different Fd concentrations. The signal amplitudes at 400 μs after the flash were measured in order to take into account all fast components of Fd reduction and were plotted versus the Fd concentration (Figure 2, middle part). Data were fitted assuming a simple binding equilibrium between Fd and PSI. A dissociation constant of 0.29 μM was thus derived, which is similar to the value obtained in untreated PSI (Table 1; *40*, *41*). Kinetics of ferredoxin reduction were recorded from 460 to 600 nm with the reconstituted sample, thus allowing derivation of the spectrum of the above process. The amplitudes of the signals were also measured at 400 μs after the flash, resulting in a spectrum which is shown in the lower part of Figure 2 (closed circles). Absorption decreases are plotted as positive signals for easier comparison with earlier published decay-associated spectra. The observed spectrum can be compared to the calculated spectrum for electron transfer from $(F_A, F_B)^-$ to Fd (open squares) (*41*) (see legend for calibration of the vertical scale and normalization procedures). The high similarity in spectral shapes clearly shows that the observed spectrum corresponds to electron transfer from a [4Fe-4S] cluster of PSI to the [2Fe-2S] cluster of Fd. However its amplitude is only 50% of that expected if all slowly relaxing PSI was able to rapidly reduce Fd. This can be partly ascribed to reaction centers containing only F_A after reconstitution: from the EPR study of reconstituted PSI (see above), such reaction centers correspond to about one-sixth of reaction centers with slowly relaxing $P700^+$. Therefore some reaction centers containing both F_A and F_B seem unable to

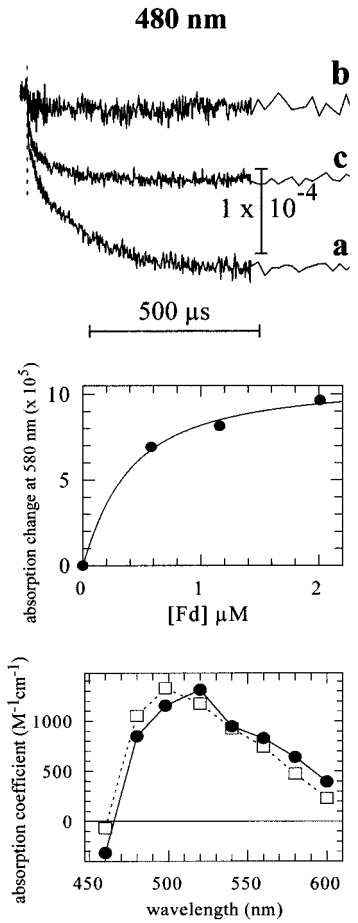

FIGURE 2: Upper part: differences between flash-induced absorption changes measured at 480 nm in the presence and in the absence of soluble Fd from *Synechocystis* 6803. Experimental conditions are identical to those of Figure 1. Curve a, control PSI (1.62 μM Fd); curve b, $HgCl_2$-treated PSI (2.01 μM Fd); and curve c, reconstituted PSI (1.73 μM Fd). The PSI concentration corresponding to slowly relaxing $P700^+$ is 0.15 μM in all cases. Middle part: dependence of the 580 nm flash-induced absorption changes due to Fd reduction by reconstituted PSI measured 400 μs after the flash on the Fd concentration. The signal amplitude was measured on difference kinetics similar to curve c of the upper part. The signal is negative and absolute values are shown here. The data were fitted considering a simple binding equilibrium between PSI and Fd, resulting in a dissociation constant K_d of 0.29 μM. Lower part: full circles, spectrum due to Fd reduction measured between 460 and 600 nm with reconstituted PSI (0.18 μM of slowly relaxing $P700^+$; 1.73 μM of Fd). The signals measured 400 μs after the flash in kinetics similar to curve c of the upper part have been taken into account and were multiplied by (1/0.85). Such a multiplication is justified by the fact that, when assuming a K_d of 0.29 μM, only 85% of PSI has Fd bound under the conditions used for measuring the spectrum. The vertical scale is calculated by comparison of the signal amplitudes to that of slowly relaxing $P700^+$, which was measured at 820 nm on the same sample ($\Delta\epsilon$ = 6500 M^{-1} cm^{-1}). The calculated spectrum for electron transfer from $(F_A, F_B)^-$ to Fd is also shown (open squares, *41*). For comparison of the spectral shapes, this calculated spectrum was multiplied by a factor of 0.51 so that both spectra exhibit similar areas between 460 and 600 nm.

reduce rapidly Fd. This subpopulation (about 30% of centers with slowly relaxing $P700^+$) may be devoid of PsaD and (or) PsaE, as SDS−PAGE of reconstituted PSI indicates a partial loss of these subunits (not shown). Such reaction centers are not expected to give fast kinetics of Fd reduction (*47*, *48*). Despite this, our data unambiguously show that reconstitution of F_B restores fast kinetics of Fd reduction, thus emphasizing that, in a significant proportion of PSI reaction centers, the $HgCl_2$ treatment did not result in irreversible damaging effects.

Photovoltage Measurements on $HgCl_2$-Treated Membranes. To test whether reduction of F_A is impaired in the $HgCl_2$-treated samples, photovoltage kinetic profiles were obtained for native, $HgCl_2$-treated, and urea-treated (both F_A and F_B removed) OGP membranes (Figure 3A). For these measurements, a PSI preparation different from that used in absorption experiments was used (OGP versus β-DM). Solubilization by OGP leads to large membrane fragments which can be properly oriented for photovoltage measurements. As no kinetic difference was observed between the control and the $HgCl_2$-treated samples (see below), no attempt was made to reconstitute F_B in the OGP PSI preparation. The photovoltage technique can be used to record the kinetics of electrogenic phases of photoinduced electron transfer. It can also provide structural information, as the signal amplitudes of the different components reflect the dielectrically weighted transmembrane distances between the cofactors involved in electron transfer (*49*). It has been previously shown that the rising phase, which is observed in the control sample with a time constant of 210 ns, reflects electron transfer from the quinone A_1 to (F_A, F_B) (*39*). This component follows a much faster rise which is not resolved in the present experiment and which corresponds to the initial charge separation between $P700^+$ and A_0^- followed by electron transfer from A_0^- to A_1, thus leading to the radical pair ($P700^+-A_1^-$) formed within 100 ps (*50*). It has been also shown that a rising component with similar kinetics (210 ns) but a smaller amplitude is observed after destruction of F_A and F_B (urea-treated sample). This was interpreted as electron transfer from A_1^- to F_X (lifetime of 210 ns) being slower than electron transfer from F_X^- to (F_A, F_B), and an upper value of 50 ns was tentatively deduced for the time constant of this last step.

In principle, a change in the relative transmembrane distance between F_X and the terminal acceptor might be detectable as a change in the relative amplitude of the 210 ns phase. In the $HgCl_2$-treated sample, a component with similar kinetics is observed but with an amplitude reduced by 25% compared to the control (the relative amplitudes of the 210 ns component, i.e., the amplitude ratios of this component to the fast unresolved signals, are 0.52, 0.39, and 0.23 for the control, $HgCl_2$-treated, and urea-treated samples, respectively). The loss of amplitude in the $HgCl_2$-treated sample (which shows no detectable amounts of F_B in EPR measurements) can be mainly attributed to 30% of reaction centers with both F_A and F_B destroyed, as measured from flash-absorption kinetics at 820 nm. In Figure 3B are shown as vertical bars the relative electrogenic amplitudes which are expected to be observed for electron transfer from A_1^- to F_A in four possible cases after correction for 30% destroyed F_A. First, the electrogenicity observed in the control sample might correspond to reduction of the proximal cluster (cluster F_I; left two bars) or the distal cluster (cluster F_{II}; right two bars). These might be considered as extreme cases of the electron being shared between F_I and F_{II} in the intact sample at room temperature due to thermodynamic equilibrium between the states (F_I^-, F_{II}) and (F_I, F_{II}^-). Alternatively the transfer $F_I \rightarrow F_{II}$ might show little electrogenicity (due to a higher effective dielectric constant) or

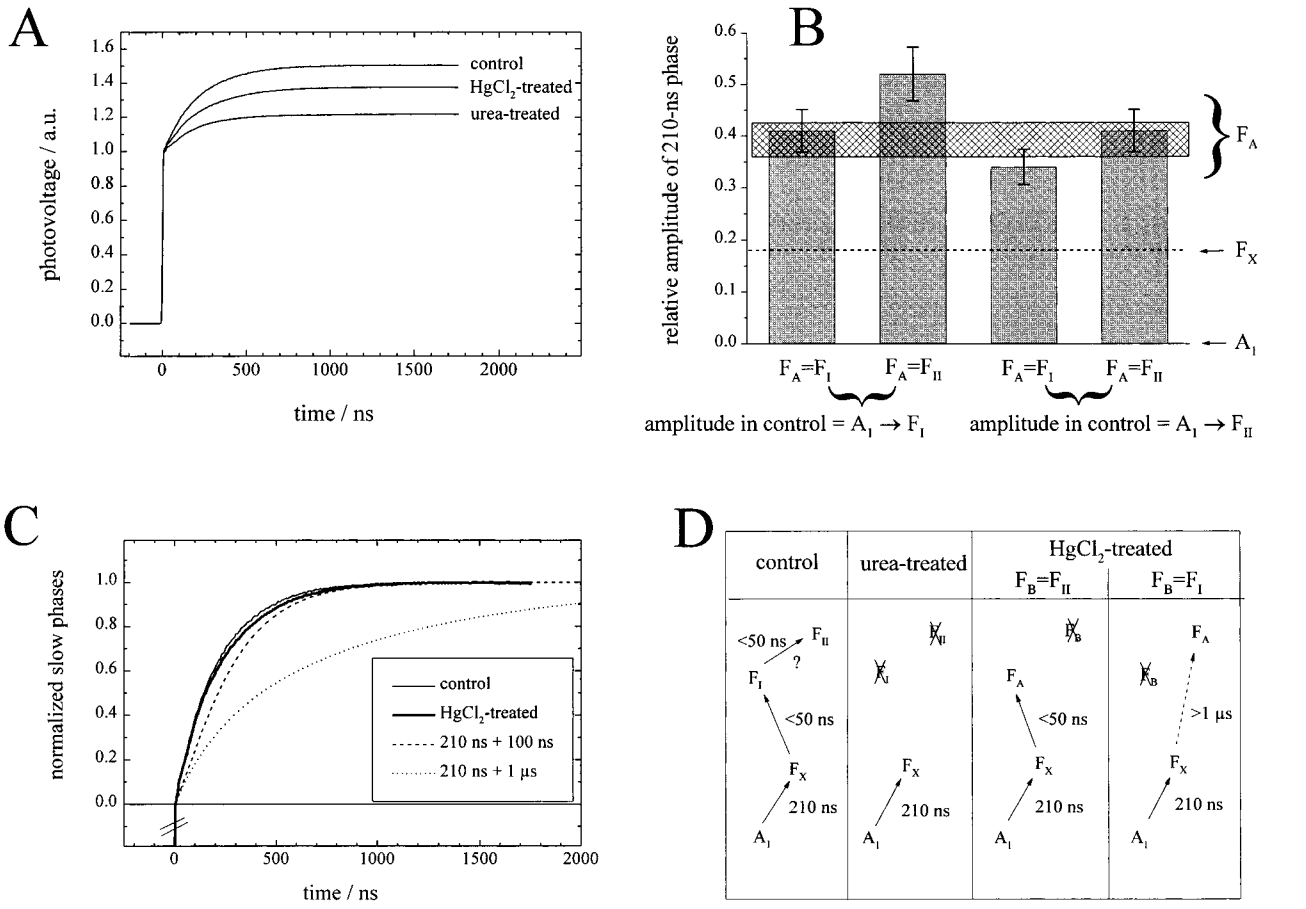

FIGURE 3: (A) Photovoltage response of PSI membranes in the nanosecond time range: untreated sample (control), after $HgCl_2$ treatment ($HgCl_2$-treated), and after treatment to remove F_A and F_B (urea-treated). For a clearer presentation, an exponential decay due to ionic relaxations present in the original data was deconvoluted. The traces were normalized to match the relative ampitude of the unresolved fast rising phase, which is due to electron transfer from P700 to A_1. A kinetic analysis yields an exponential time constant of 210 ± 10 ns for the slow positive phase in all samples with relative amplitudes of 0.52, 0.39, and 0.23, respectively. The absence of F_B in the $HgCl_2$-treated samples was tested by EPR and by flash-induced absorption changes at 820 nm. According to these data, 30% of F_A clusters were destroyed by this treatment, showing a decay faster than 30 ms, and 5% of F_X was also lost (decay faster than 100 μs). (B) Comparison of the relative amplitude of the 210 ns phase as measured in $HgCl_2$-treated sample (hatched horizontal bar) and the amplitudes expected for different scenarios (vertical bars). Left two bars, the electrogenicity observed for the 210 ns phase in control samples corresponds to the proximal Fe−S cluster F_I; right two bars: it corresponds to the distal Fe−S cluster F_{II}. For both possibilities the terminal acceptor in $HgCl_2$-treated samples, F_A, can be the proximal or the distal Fe−S cluster. The loss in $HgCl_2$-treated samples of 30% of F_A and 5% of F_X has been taken into account in the calculation of the expected amplitudes. (C) Comparison of the kinetics of the slow phase of photovoltage for control and $HgCl_2$-treated samples. The amplitudes of both phases were normalized to equal size. Both kinetics are well fitted by a single-exponential phase with a time constant of 210 ± 10 ns (not shown). Also presented are calculated kinetics based on a two-step sequential reaction scheme with a first phase due to electron transfer from A_1 to F_X (210 ns; relative electrogenicity 36%) and a second phase due to electron transfer from F_X to F_A or F_B (100 ns, dashed line, or 1 μs, dotted line; relative electrogenicity 64%). The relative electrogenicities of the electron transfer steps are those observed in the present study (urea-treated versus control) and are similar to those found previously (*39*). (D) schematic drawing of the reaction pathways in control, urea-treated, and $HgCl_2$-treated samples.

occur with kinetics so slow that it cannot be detected on this time scale (*51*). This last possibility appears less likely because Fd can be reduced by F_{II} in less than 1 μs (faster phase of reduction, *40*). In both cases mentioned above the terminal acceptor in $HgCl_2$-treated samples (F_A) might be the proximal ($F_A = F_I$) or the distal cluster ($F_A = F_{II}$). Neglecting for the moment kinetic arguments, it can be seen, that three out of four possibilities yield similar relative amplitudes of the 210 ns phase which, within the experimental error, are compatible with the experimentally determined relative amplitude (hatched horizontal bar). Even the second scenario cannot be excluded as the calculated amplitude assumes an extreme case of complete electron localization on F_I (in control) and a dielectric constant similar for both $F_X \rightarrow F_I$ and $F_I \rightarrow F_{II}$ steps. Therefore, when taking into account the partial loss of F_A after $HgCl_2$ treatment, no clear effect of the $HgCl_2$ treatment on the electrogenicity of the 210 ns phase can be deduced.

However, when the kinetics of the slow photoelectric phases in control samples and that of $HgCl_2$-treated samples are compared (Figure 3C) it appears clearly that F_B removal does not significantly alter the reduction kinetics of F_A, supporting a lifetime of less than 50 ns for this reaction which, in the absence of F_B, is still kinetically controlled by electron transfer from A_1 to F_X. This is demonstrated in Figure 3C by comparing the experimental data with two simulated kinetics which are calculated under the assumption of a 210 ns kinetics of electron transfer from A_1^- to F_X followed by electron transfer from F_X^- to F_A with either 100 ns (dashed line) or 1 μs (dotted line; see Figure 3D for a schematic representation of the reaction sequences in the different samples).

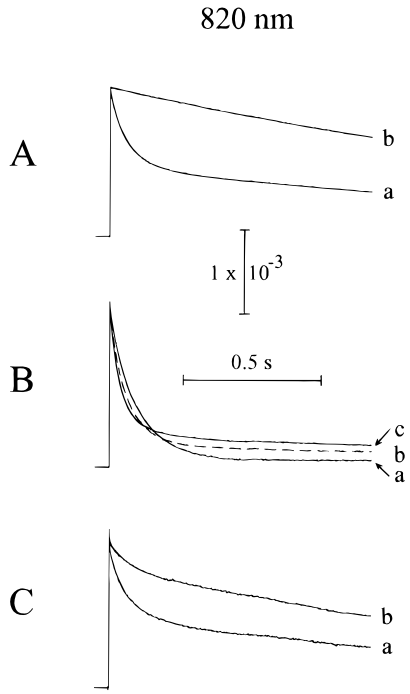

FIGURE 4: Flash-induced absorption changes at 820 nm on a 1 s time scale with control (part A), $HgCl_2$-treated (part B), and reconstituted PSI (part C) in the absence (traces a) or presence (traces b and c) of Fd from *Synechocystis* 6803. The experimental conditions are identical to those of Figure 1 (except 1 flash every 20 s and averages of 16 experiments for each trace). Fd concentrations: 1.25 μM for trace b of part A, 0.93 and 4.23 μM for traces b and c of part B, respectively, 2.01 μM for trace b of part C. All signals correspond to the same concentrations of slowly decaying reaction centers (0.24 μM), containing at least one terminal acceptor F_A or F_B.

Effect of Fd Addition on P700$^+$ Decay in Control, $HgCl_2$-Treated, and Reconstituted Samples. Figure 4 shows the laser flash-induced absorption changes at 820 nm ascribed to $P700^+$ decay in control (part A), $HgCl_2$-treated (part B), and reconstituted (part C) samples in the absence (traces a) or in the presence of ferredoxin (traces b and c). All traces correspond to the same concentration of slowly decaying $P700^+$ ($t_{1/2} \gg 1$ ms), therefore involving only PSI reaction centers containing at least one terminal acceptor F_A and F_B, when present. In $HgCl_2$-treated and reconstituted reaction centers, $P700^+$ exhibits a much faster initial decay ($t_{1/2} \leq 1$ ms; see above and Figure 1) which is not resolved in the present experiment (1 s full time scale) and which is not further considered below. All traces shown in Figure 4 can be satisfactorily fitted with two exponential components. The faster of these two components, thereafter called slow phase, corresponds to a recombination process between $P700^+$ and F_A^- [or $(F_A, F_B)^-$ when F_B is present]. The slower of the two components, thereafter called very slow phase, is due to $P700^+$ reduction by reduced 2,6-dichlorophenolindophenol (DCPIP) in reaction centers in which electron has escaped from the terminal acceptor F_A^- [or $(F_A, F_B)^-$] to an exogenous acceptor (*48*). Concerning the observed rate of $P700^+$ recombination (slow phase), it is governed by the decay of the reduced terminal acceptor, which disappears with a rate $k_{obs} = k_r + k_e$, with k_r and k_e being the rate constants of recombination and escape, respectively. Moreover, the amplitude ratio between the very slow and the slow phases of $P700^+$ decay is equal to k_e/k_r (i.e., the percentage of very slow phase is $k_e/(k_e+k_r)$). Knowing both parameters (observed rate of slow phase, amplitude ratio of the two phases) therefore allows calculation of the rate constants k_r and k_e, which are given for the three types of PSI in Table 1. As can be directly inferred from comparison of traces a, the escape process is rather inefficient in the $HgCl_2$-treated sample compared to the control and reconstituted samples. This is due to a large difference in the escape rates between the $HgCl_2$-treated and the two other samples (0.7 s^{-1} versus 6−8 s^{-1}). By contrast, the recombination rates are similar in all three samples (between 7.7 and 10.3 s^{-1}). The observations of a much less efficient escape process after destruction of F_B and a significant recovery of this process after reconstitution of F_B indicate that escape occurs mostly from cluster F_B.

After addition of Fd, the $P700^+$ decay is much slower both in the control and in the reconstituted sample. In the control sample (trace b, 1.25 μM Fd), $P700^+$ decay is monophasic and can be completely ascribed to reduction by reduced DCPIP, in line with a fast and efficient process of ferredoxin reduction (*40*, *41*). In the reconstituted sample (trace b, 2.01 μM Fd), 83% of $P700^+$ decay is very slow (due to reduction by reduced DCPIP), whereas the slow component (17%; $k_{obs} \approx 19$ s^{-1}) reflects a recombination process. Increasing the Fd concentration does not allow the amplitude of the recombination process to decrease significantly (16% of absorption decay with a Fd concentration of 4.2 μM). These observations are consistent with the absorption changes measured in the visible region after reconstitution, indicating that fast reduction of ferredoxin is observable in only 50% of PSI containing a terminal acceptor (see above) and with the Fd reduction behavior of $HgCl_2$-treated PSI (see below). It has been shown above that 50% of reaction centers with slowly decaying $P700^+$ are transferring rapidly (submicrosecond and microsecond time ranges) an electron to Fd. The kinetic behavior of this subpopulation should therefore be similar to that of control PSI (trace b), i.e., a very slow decay due to reduction by reduced DCPIP. In the other half of reaction centers, kinetics parameters are difficult to evaluate due to the heterogeneity of this subpopulation (some reaction centers containing only F_A, others containing both F_A and F_B but not able to reduce rapidly Fd; see discussion above).

Fd reduction by the $HgCl_2$-treated reaction centers (Figure 4B) deserves a more detailed analysis. As in its absence, kinetics of $P700^+$ decay in the presence of Fd can be satisfactorily fitted by two exponential components. When compared to trace a (no Fd), addition of Fd (0.93 and 4.23 μM for traces b and c, respectively) increases the amount of stable $P700^+$ (amplitude of very slow phase) as well as the rate k_{obs} of the slow component. Both parameters (stable $P700^+$ and k_{obs}) increase with Fd concentration (Figure 5, parts A and B). These increases can be ascribed to slow electron transfer from F_A to Fd (in tens or hundreds of milliseconds). Both dependences saturate at high ferredoxin concentrations, as can be seen from the similar kinetic patterns for Fd concentrations of 2 and 4 μM. Such observations cannot be explained by a diffusion-limited reduction of Fd but rather imply the formation of a complex between $HgCl_2$-treated PSI and Fd with a dissociation constant in the micromolar range together with a limiting electron-transfer step. For a quantitative analysis, we assume that formation and dissociation of such a complex are fast

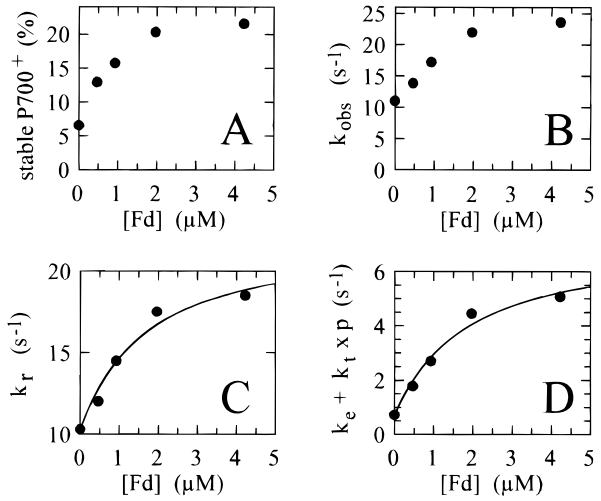

FIGURE 5: Kinetic parameters in $HgCl_2$-treated sample. These parameters were derived from kinetics as those shown in part B of Figure 4: the kinetics on a 1 s time scale (not taking into account data during the first 5 ms after the flash) was fitted with two exponential components. Stable $P700^+$ (part A) is measured from the amplitude of the slower component, named "very slow component" in the text ($t_{1/2} \approx 1.2$ s; independent of Fd concentration) which results from $P700^+$ reduction by reduced DCPIP. The percentage is calculated by reference to the sum of amplitudes of the two exponential components. k_{obs} (part B) is the rate of the faster component, named "slow component" in the text; both parameters (stable $P700^+$ and k_{obs}) were measured as a function of Fd concentration. For a given ferredoxin concentration, the two above numbers (amount of stable $P700^+$ and k_{obs} of faster component) were used to derive the recombination and forward electron-transfer rates, named "k_r" and "$(k_e + k_t p)$", respectively. These rates were derived from the following identities: $k_{obs} = k_e + k_t p + k_r$ and percentage of stable $P700^+ = (k_e + k_t p)/(k_e + k_t p + k_r)$ (see the text). The dependences of k_r and $(k_e + k_t p)$ versus Fd concentrations are shown in parts C and D, respectively, and were fitted by assuming a fast binding equilibrium between PSI and ferredoxin (continuous lines in parts C and D; see the text). Rate values obtained without ferredoxin were taken as fixed values during the fitting procedures ($k_{rfree} = 10.3\ s^{-1}$ and $k_e = 0.7\ s^{-1}$). The dissociation constant K_d, the electron-transfer rate k_t, and the recombination rate within the complex $k_{rcomplex}$ were free parameters. The fitting procedures resulted in the following values: part C, $k_{rcomplex} = 22.1\ s^{-1}$ and $K_d = 1.5\ \mu M$; part D, $k_t = 6.3\ s^{-1}$ and $K_d = 1.7\ \mu M$.

processes compared to the observed electron-transfer rates ($<25\ s^{-1}$). With this assumption, the rate of Fd reduction will be $(k_t p)$, k_t being the first-order rate of electron transfer within the PSI−Fd complex and p being the proportion of PSI forming a complex with Fd. In line with the above paragraphs, the amount of stable $P700^+$ should be equal to the ratio $(k_e + k_t p)/(k_e + k_t p + k_r)$, whereas the rate of the faster component is $(k_e + k_t p + k_r)$ (k_e, escape rate; k_r, recombination rate). This allows derivation of k_r and $(k_e + k_t p)$ for each ferredoxin concentration (Figure 5, parts C and D). An example of such a calculation is given in Table 1 for 2 μM Fd. According to what precedes, $(k_e + k_t p)$ increases with the Fd concentration as the proportion p of complexes increases. A less expected result is the increase of k_r with the Fd concentration. The recombination rate appears to be dependent upon complex formation and must therefore be written as $k_r = k_{rfree}(1 - p) + k_{rcomplex} p$ ($k_{rcomplex}$ and k_{rfree}, recombination rates in PSI binding and not binding Fd, respectively). The two lower curves of Figure 5 were thus fitted assuming a simple binding equilibrium between $HgCl_2$-treated PSI and Fd which governs the proportion p of PSI/Fd complex at a given Fd concentration. The following values (Table 1) resulted from such a fitting procedure assuming k_{rfree} and k_e as fixed values (10.3 and $0.7\ s^{-1}$ respectively):

From the dependence of k_r, K_d (dissociation constant) = 1.5 μM and $k_{rcomplex}$ (recombination rate within the complex) = $22.1\ s^{-1}$.

From the dependence of $(k_e + k_t p)$, $K_d = 1.7\ \mu M$ and k_t (rate of electron transfer within the complex) = $6.3\ s^{-1}$.

Assuming that the second-order rate constant is similar to that of the control ($\approx 3.5 \times 10^8\ M^{-1}\ s^{-1}$, *40*) and with $K_d = 1.6\ \mu M$, the rate of Fd binding to PSI and the dissociation rate ($k_{off} = k_{on} K_d$) can be calculated ($350\ s^{-1}$ for 1 μM Fd and $560\ s^{-1}$, respectively). These numbers are 1−2 orders of magnitude larger than the preceding calculated electron-transfer rates, therefore justifying the above assumption of a fast binding equilibrium between Fd and PSI. Two main conclusions must be emphasized from the study of Fd reduction by $HgCl_2$-treated PSI: first, the electron-transfer rate within the PSI/Fd complex is very small in the absence of F_B ($6.3\ s^{-1}$), whereas the Fd dissociation constant is reduced only 3−4 times compared to control PSI (see Table 1); second, the recombination rate within the complex is faster than the recombination rate in the absence of ferredoxin ($22.1\ s^{-1}$ versus $10.3\ s^{-1}$). This can be tentatively ascribed to an electrostatic effect due to the large number of negative charges carried by Fd.

DISCUSSION

The main purpose of this study concerns the elucidation of the electron transfer pathway in the acceptor side of PSI, especially the determination of the specific role played by each of the two iron−sulfur clusters of the subunit PsaC, which belongs to the family of 2[4Fe-4S] ferredoxins. It has been already recognized that, in the absence of F_B, F_A is reduced at room temperature with a yield close to unity after a flash excitation (*21*, *22*, *24*). These observations show that F_A reduction is faster than 1 ms, as it needs to compete efficiently with the recombination reaction from F_X^- ($t_{1/2} \approx$ 1 ms). Our photovoltage measurements extend considerably these observations by allowing derivation of an upper value for the lifetime of F_A reduction in the absence of F_B. These data show that, in the absence of F_B, the reduction of F_A is still kinetically controlled by electron transfer from A_1 to F_X and they support a lifetime of less than 50 ns for electron transfer from F_X to F_A. Considering the present uncertainties in the edge-to-edge distances between iron−sulfur clusters of PSI and by using an empirical formula for electron transfer (*52*), it has been calculated that the electron-transfer rate between F_X and the distal cluster should be comprised between 2×10^3 and $2 \times 10^6\ s^{-1}$ (*2*, *53*). It has been also stressed that these rates are overestimated so that the upper value is rather stringent, thus meaning that the time constant for direct electron transfer from F_X to the distal cluster is most certainly larger than 500 ns. Therefore, the fast kinetics of F_A reduction in the absence of F_B strongly supports F_A as the proximal cluster.

We also measured for the first time Fd reduction in the absence of F_B. Whereas this process is too slow to be recorded directly in the visible region, it can be recorded through the $P700^+$ decay, due to the fact that both processes

of recombination between $P700^+$ and F_A^- and of Fd reduction occur in the same time range. Our results indicate that no large structural change is occurring following F_B destruction as Fd binding is only weakly impaired in $HgCl_2$-treated PSI. Moreover, it was possible to derive the rate of Fd reduction within the PSI/Fd complex. A value of 6.3 s^{-1} was thus found which is several orders of magnitude slower that the rate measured with intact PSI. As the binding properties of Fd are only weakly affected after F_B removal, it seems rather unlikely that such a huge change is due to the fact that Fd binds in a site different from its normal one. Therefore, the observed slow rate can be more readily explained by F_A being the cluster proximal to the membrane plane and thus relatively far from Fd (*28*). The Fd reduction rate is also found to be smaller than the recombination rate from F_A^- (22.1 s^{-1} within the PSI/Fd complex), thus leading to a weak efficiency (≈25%) of electron transfer from F_A^- to Fd. This poor efficiency appears to be the main factor leading to a decreased $NADP^+$ photoreduction in the absence of F_B. In previous reports, $NADP^+$ photoreduction by $HgCl_2$-treated PSI is reported to be 5−13% that of the control (*23*−*25*). These values are somewhat smaller than the efficiency of Fd reduction which is observed in the present experiments. These differences may be due to different effects: (a) Fd reduction is not only inefficient but is also very slow, so the inhibition effect may be larger in experiments implying multiple turnovers which could be kinetically limited by Fd reduction. However, a simple calculation shows that a limiting rate of 6.3 s^{-1} for Fd reduction corresponds approximately to a rate of $NADP^+$ photoreduction of 65 μmol/(mg of chlorophyll·h) for an antenna size of 200 chlorophylls per P700 (and twice more for an antenna size of 100). These values are higher than those previously observed with $HgCl_2$-treated PSI preparations. So other explanations must be sought: (b) the Fd amount may be not saturating, due to some loss in affinity after treatment (a factor of 3−4 is found in the present study) and (or) due to the use of spinach Fd which has been found to bind less efficiently to PSI than Fd from *Synechocystis* 6803 (*41*). (c) The Fd reduction rate in the absence of F_B is so small (6.3 s^{-1}) that Fd may be partially reoxidized by oxygen before it can transfer an electron to ferredoxin-$NADP^+$-reductase.

The kinetic analysis of $P700^+$ decay in the absence of F_B also suggests that charge recombination between $P700^+$ and F_A^- is accelerated when Fd is bound. Though the pathway of charge recombination between $P700^+$ and $(F_A, F_B)^-$ (or F_A^- in the $HgCl_2$-treated sample) is not yet unambiguously established (*2*), a direct recombination process seems highly unlikely owing to the huge distance separating $P700^+$ and the proximal cluster (more than 45 Å). It appears much more likely that recombination proceeds more efficiently through population of charge-separated states involving primary or secondary acceptors. Under this assumption, and whatever the precise pathway of recombination is, the recombination rate will be governed by the difference in midpoint redox potential between F_A and the acceptor which is reduced during the recombination process. The 2.15 increase in recombination rate which is observed between free PSI and the PSI/Fd complex can be translated into a 20 mV decrease in the above redox potential difference.

The overall preservation of the Fd binding properties indicates that the structure of the stromal part of PSI is not strongly affected by F_B destruction. This contrasts with the observation that both clusters of 2[4Fe-4S] bacterial Fds are essential for maintaining their structures (*54*). Such a structural tolerance toward F_B destruction may be due to the stabilizing roles of the peripheral subunits PsaD and PsaE of PSI. The relative structural integrity of F_B-depleted PSI is in line with previous data showing that Fd can be cross-linked to $HgCl_2$-treated PSI (*24*) and with successful reconstitution experiments (*25* and this report). Although the present data indicate that, in our hands, reconstitution of F_B is only partial, in line with a previous report (*24*), this partial reconstitution is largely sufficient for interpreting conclusively our kinetic data. Taken together, these data support a linear scheme of electron transfer involving sequentially F_X, F_A, F_B, and Fd, as summarized in Figure 6, which is based upon the structural data concerning the positions of the three different iron−sulfur clusters of PSI (*6*).

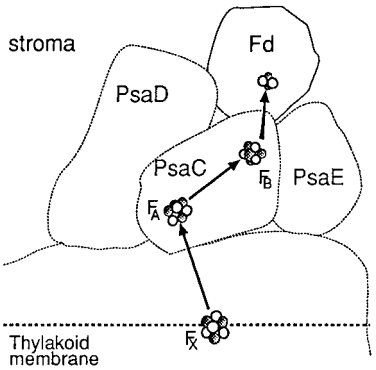

FIGURE 6: Arrangement of the iron−sulfur clusters in PSI and the electron-transfer pathway at its acceptor side. According to the present data, F_A is the cluster which is proximal to F_X and, according to cross-linking experiments and electron microscopy of deletion mutants (see e.g. *67*), it lies closer to the PsaD subunit than F_B, which is the distal cluster of PsaC and the immediate electron donor to Fd.

Recently, Mannan et al. (*17*) reported that the site-directed mutant C13D in PsaC of *Anabaena* leads to the destruction of F_B without affecting the steady-state rate of $NADP^+$ reduction in the cyanobacterial membrane. However the data shown by these authors are not internally consistent, which makes them difficult to interpret: it can be seen from Figure 3 of this work that a large part of the $P700^+$ decay can be ascribed to a recombination reaction. This means that F_A reduction is far from 100% efficient (and probably less than 40%) in the C13D mutant, so $NADP^+$ photoreduction should be necessarily affected in the mutant in the absence of a very efficient donor. Our results contrast with conclusions based on site-directed mutagenesis studies of the *psa*C gene (*29*, *30*), from which some residues or regions were claimed to be important for the interaction between the core heterodimer of PSI and the PsaC subunit. These data were taken as support for F_B being the proximal cluster (see also ref 12). The only available model of the PsaC structure is based on sequence alignment with the *Peptococcus aerogenes* soluble ferredoxin of known structure (*55*, *56*). However this sequence alignment is rather poor, except in the regions containing the cysteine ligand motifs and the α-helical parts which connect the two clusters (*29*, *56*). These last domains are the only structural determinants which are involved in the relative positioning of the two clusters. This is in line

with the observations that the relative distances and orientations of F_A and F_B are similar to those found in 2[4Fe-4S] bacterial ferredoxins (*6*, *7*, *12*, *57*), but this similarity cannot be safely extended to other parts of PsaC. All these uncertainties make rather difficult any straightforward interpretation of site-directed or deletion mutations in the regions not homologous to bacterial ferredoxins, particularly those concerning extensions in an internal loop or at the C-terminus (*29*, *30*). The above restrictions do not apply to the mutant D9R (a residue close to F_B) of PsaC which is less efficient than wild type in reconstitution of core PSI (devoid of stromal subunits) (*30*). This observation is difficult to reconcile with our results, and further work is needed to resolve this discrepancy.

The functional properties of 2[4Fe-4S] ferredoxins are only poorly understood, despite recent progress. Intramolecular electron transfer between the two clusters has been characterized and can be very different from one ferredoxin to another (*58*−*62*). Moreover, it is not clearly known whether the two clusters are equivalent in their interactions with redox partners (*63*, *64*), although they exhibit differential reactivities toward small electron donors or oxidants (*65*, *66*). Thus PSI constitutes the only case in which both clusters are shown to be essential for the functionality of the protein. However, it is still unknown why it is advantageous for PSI to use two different clusters of similar redox potential as terminal acceptors. The localization of F_A and F_B clusters afforded by the present study is a prerequisite for clarifying this issue.

ACKNOWLEDGMENT

A. D.-Q. thanks Dr. B. Lagoutte for discussions and Dr. P. Mathis for support.

REFERENCES

1. Golbeck, J. H. (1994) in *The Molecular Biology of Cyanobacteria* (Bryant, D. A., Ed.), pp 319−360, Kluwer Academic Publishers: Dordrecht.
2. Brettel, K. (1997) *Biochim. Biophys. Acta 1318*, 322−373.
3. Lüneberg, J., Fromme, P., Jekow, P., and Schlodder, E. (1994) *FEBS Lett. 338*, 197−202.
4. Moënne-Loccoz, P., Heathcote, P., Maclachlan, D. J., Berry, M. C., Davis, I. H., and Evans, M. C. W. (1994) *Biochemistry 33*, 10037−10042.
5. Van der Est, A., Bock, C., Golbeck, J., Brettel, K., Sétif, P., and Stehlik, D. (1994) *Biochemistry 33*, 11789−11797.
6. Schubert, W.-D., Klukas, O., Krauss, N., Saenger, W., Fromme, P., and Witt, H. T. (1997) *J. Mol. Biol.* 272, 741−769.
7. Krauss, N., Hinrichs, W., Witt, I., Fromme, P., Pritzkow, W., Dauter, Z., Betzel, C., Wilson, K. S., Witt, H. T., and Saenger, W. (1993) *Nature 361*, 326−331.
8. Adman, E. T., Sieker, L. C., and Jensen, L. H. (1976) *J. Biol. Chem. 251*, 3801−3806.
9. Duée, E. D., Fanchon, E., Vicat, J., Sieker, L. C., Meyer, J., and Moulis, J.-M. (1994) *J. Mol. Biol. 243*, 683−695.
10. Bertini, I., Donaire, A., Feinberg, B. A., Luchinat, C., Piccioli, M., and Yuan, H. (1995) *Eur. J. Biochem. 232*, 192−205.
11. Moulis, J.-M., Sieker, L. C., Wilson, K. S., and Dauter, Z. (1996) *Protein Sci. 5*, 1765−1775.
12. Kamlowski, A., Van der Est, A., Fromme, P., Krauss, N., Schubert, W.-D., Klukas, O., and Stehlik, D. (1997) *Biochim. Biophys. Acta 1319*, 199−213.
13. Kamlowski, A., Van der Est, A., Fromme, P., and Stehlik, D. (1997) *Biochim. Biophys. Acta 1319*, 185−198.
14. Mehari, T., Qiao, F., Scott, M. P., Nellis, D. F., Zhao, J., Bryant, D. A., and Golbeck, J. H. (1995) *J. Biol. Chem. 270*, 28108−28117.
15. Yu, L., Bryant, D. A., and Golbeck, J. H. (1995) *Biochemistry 34*, 7861−7868.
16. Yu, J., Vassiliev, I. R., Jung, Y.-S., Bryant, D. A., and Golbeck, J. H. (1995) *J. Biol. Chem. 270*, 28118−28125.
17. Mannan, R. M., He, W.-Z., Metzger, S. U., Whitmarsh, J., Malkin, R., and Pakrasi, H. B. (1996) *EMBO J. 15*, 1826−1833.
18. Jung, Y.-S., Vassiliev, I. R., Yu, J., McIntosh, L., and Golbeck, J. H. (1997) *J. Biol. Chem. 272*, 8040−8049.
19. Yu, J., Vassiliev, I. R., Jung, Y.-S., Golbeck, J. H., and McIntosh, L. (1997) *J. Biol. Chem. 272*, 8032−8039.
20. Kojima, Y., Nijomi, Y., Tsuboi, S., Hiyama, T., and Sakurai, S. (1987) *Bot. Mag. Tokyo 100*, 243−253.
21. Fujii, T., Yokoyama, E., Inoue, K., and Sakurai, H. (1990) *Biochim. Biophys. Acta 1015*, 41−48.
22. Sakurai, H., Inoue, K., Fujii, T., and Mathis, P. (1991) *Photosynth. Res. 27*, 65−71.
23. Inoue, K., Kusomoto, N., and Sakurai, H. (1992) in *Research in Photosynthesis* (Murata, N., ed.), Vol. 1, pp 577−580, Kluwer Academic Publishers: Dordrecht.
24. He, W.-Z., and Malkin, R. (1994) *Photosynth. Res. 41*, 381−388.
25. Jung, Y. S., Yu, L., and Golbeck, J. H. (1995) *Photosynth. Res. 46*, 249−255.
26. Golbeck, J. H., and Warden, J. T. (1982) *Biochim. Biophys. Acta 681*, 77−84.
27. Fromme, P., Schubert, W. D., and Krauss, N. (1994) *Biochim. Biophys. Acta 1187*, 99−105.
28. Lelong, C., Boekema, E. J., Kruip, J., Bottin, H., Rögner, M., and Sétif, P. (1996) *EMBO J. 15*, 2160−2168.
29. Naver, H., Scott, M. P., Golbeck, J. H., Møller, B. L., and Scheller, H. V. (1996) *J. Biol. Chem. 271*, 8996−9001.
30. Rodday, S. M., Do, D. T., Chynwat, V., Frank, H. A., and Biggins, J. (1996) *Biochemistry 35*, 11832−11838.
31. Bottin, H., and Sétif, P. (1991) *Biochim. Biophys. Acta 1057*, 331−336.
32. Bottin, H., and Lagoutte, B. (1992) *Biochim. Biophys. Acta 1101*, 48−56.
33. Rögner, M., Dixon, P. J., and Diner, B. A. (1990) *J. Biol. Chem. 265*, 6189−6196.
34. Kruip, J., Bald, D., Boonstra, A. F., and Rögner, M. (1993) *J. Biol. Chem. 268*, 23353−23360.
35. Porra, R. J., Thomson, W. A., and Kriedemann, P. E. (1989) *Biochim. Biophys. Acta 975*, 384−394.
36. Mathis, P., and Sétif, P. (1981) *Isr. J. Chem. 21*, 316−320.
37. Golbeck, J. H., Parrett, K. G., Mehari, T., Jones, K. L., and Brand, J. J. (1988) *FEBS Lett. 228*, 268−272.
38. Parrett, K. G., Mehari, T., and Golbeck, J. H. (1990) *Biochim. Biophys. Acta 1015*, 341−352.
39. Leibl, W., Toupance, B., and Breton, J. (1995) *Biochemistry 34*, 10237−10244.
40. Sétif, P. Q. Y., and Bottin, H. (1994) *Biochemistry 33*, 8495−8504.
41. Sétif, P. Q. Y., and Bottin, H. (1995) *Biochemistry 34*, 9059−9070.
42. Warren, P. V., Golbeck, J. H., and Warden, J. T. (1993) *Biochemistry 32*, 849−857.
43. Brettel, K., and Golbeck, J. H. (1995) *Photosynth. Res. 45*, 183−193.
44. Golbeck, J. H., and Cornelius, J. M. (1986) *Biochim. Biophys. Acta 849*, 16−24.
45. Parrett, K. G., Mehari, T., Warren, P. G., and Golbeck, J. H. (1989) *Biochim. Biophys. Acta 973*, 324−332.
46. Beinert, H., and Kennedy, M. C. (1989) *Eur. J. Biochem. 186*, 5−15.
47. Hanley, J., Sétif, P., Bottin, H., and Lagoutte, B. (1996) *Biochemistry 35*, 8563−8571.
48. Rousseau, F., Sétif, P., and Lagoutte, B. (1993) *EMBO J. 12*, 1755−1765.
49. Skulachev, V. P. (1987) *FEBS Lett. 225*, 1−5.
50. Hecks, B., Wulf, K., Breton, J., Leibl, W., and Trissl, H.-W. (1994) *Biochemistry 33*, 8619−8624.
51. Sigfridsson, K., Hansson, Ö and Brzezinski, P. (1995) *Proc. Natl. Acad. Sci. U.S.A.* 92, 3458−3462.

52. Moser, C. C., and Dutton, P. L. (1992) *Biochim. Biophys. Acta 1101*, 171−176.
53. Sétif, P., and Brettel, K. (1993) *Biochemistry 32*, 7846−7854.
54. Moulis, J.-M., Davasse, V., Golinelli, M.-P., Meyer, J., and Quinkal, I. (1996) *J. Biol. Inorg. Chem. 1*, 2−14.
55. Dunn, P. P. J., and Gray, J. C. (1988) *Plant Mol. Biol. 11*, 311−319.
56. Oh-Oka, H., Takahashi, Y., Kuriyama, K., Saeki, K., and Matsubara, H. (1988) *J. Biochem. 103*, 962−968.
57. Guigliarelli, B., Guillaussier, J., More, C., Sétif, P., Bottin, H., and Bertrand, P. (1993) *J. Biol. Chem. 15*, 900−908.
58. Gaillard, J., Moulis, J. M., and Meyer, J. (1987) *Inorg. Chem. 26*, 320−324.
59. Gaillard, J., Quinkal, I., and Moulis, J. M. (1993) *Biochemistry 32*, 9881-9887.
60. Bertini, I., Capozzi, F., Luchinat, C., Piccioli, M., and Vila, A. J. (1994) *J. Am. Chem. Soc. 116*, 651−660.
61. Huber, J. G., Gaillard, J., and Moulis, J.-M. (1995) *Biochemistry 34*, 194−205.
62. Kyritsis, P., Huber, J. G., Quinkal, I., Gaillard, J., and Moulis, J.-M. (1997) *Biochemistry 36*, 7839−7846.
63. Blanchard, L., Payan, F., Qian, M., Haser, R., Nouilly, M., Bruschi, M., and Guerlesquin, F. (1993) *Biochim. Biophys. Acta 1144*, 125−133.
64. Quinkal, I., Davasse, V., Gaillard, J., and Moulis, J.-M. (1994) *Protein Eng. 7*, 681−687.
65. Navarro, J. A., Cheddar, G., and Tollin, G. (1989) *Biochemistry 28*, 6057−6065.
66. Bertini, I., Briganti, F., Calzolai, L., Messori, L., and Scozzafava,A. (1993) *FEBS Lett. 332*, 268−272.
67. Kruip, J., Chitnis, P. R., Lagoutte, B., Rögner, M., and Boekema, E. J. (1997) *J. Biol. Chem. 272*, 17061−17069.

BI972469L